RSC Advances

ROYAL SOCIETY OF CHEMISTRY

www.rsc.org/advances

Mesoporous carbonaceous materials prepared from used cigarette filters for efficient phenol adsorption and CO_2 capture

Aibing Chen [a*], Yonglei Li [a], Yifeng Yu [a], Yuetong Li [a], Linsong Zhang [b*], Haijun Lv [a], Lei Liu [a]

[a] *College of Chemistry and Pharmaceutical Engineering, Hebei University of Science and Technology, Shijiazhuang 050018, PR China*

[b] *Department of Resources and Environmental Engineering, Xingtai Polytechnic College, Xingtai 054000, PR China*

ABSTRACT

Mesoporous carbonaceous materials (MCMs) with 2-D hexagonal (*p6mm*) are synthesized through evaporation induced self-assembly on the surface of cigarette filters by using phenol/formaldehyde resol as a carbon precursor, triblock copolymer F127 as the template and cigarette filters as the matrix scaffold. The obtained MCMs incorporate the advantages of cigarette filters and phenol/formaldehyde resol, which results in enhanced performance for phenol adsorption and CO_2 capture. X-ray diffraction and transmission electron microscopy results indicate that the obtained carbon materials have an ordered *p6mm* mesostructure and good thermal stability. The MCMs possess uniform pore size (5.1 nm), large surface area (526 m^2 g^{-1}) and pore volume (0.39 cm^3 g^{-1}), as well as exhibit a considerable phenol adsorption (261.7 mg

* *Corresponding author: Tel/Fax: +86 311 8863 2183. E-mail address:chen_ab@163.com (A. B. Chen).*

* *Corresponding author: Tel/Fax: +86 319 2273354. E-mail address:ls03104126@126.com (L. S. Zhang).*

g^{-1}) and CO_2 capture (2.48 mmol g^{-1}).

Key words: cigarettes filters; mesoporous carbon; phenol adsorption; CO_2 capture

1. Introduction

A large amount of cigarettes are consumed around the world every year, in most cases, the filters are thrown away. Disposed cigarette filters are one of the biggest solid wastes produced. Much attention has to be paid for the reason of around 766,571 metric tons of cigarette filters produced each year, which pose significant environmental contamination [1]. Environmental hazards may be resulted from the leaching of toxic components from the disposed cigarette filters. They will expose the environment to not only the heavy metals but also the ethyl phenol and pesticide residues [2]. Cigarette filters made of cellulose acetate contain a high degree of carbon atoms, and can potentially be nominated as the initial scaffold materials for preparation of porous carbon [3]. Polarz et al. obtained the carbon materials by carbonizing cigarette filters at 1000 °C for 7 h with a temperature tamp of 1 °C min^{-1}, and studied the carbonization of cigarette filters in the limited carbonization conditions [4]. Unfortunately, only 262 m^2 g^{-1} BET specific surface area with a porosity volume of 0.21 cm^3 g^{-1} was obtained.

Ordered mesoporous carbons (OMCs) have received considerable attention owing to their large surface area, tunable pore structure, uniform and adjustable pore size, and mechanical stability [5]. These properties make them ideal candidates for application in adsorption [6-9], supercapacitors [8, 9], and catalysis [10]. In general, a nanocasting strategy is adopted to fabricate ordered mesoporous materials by

employing nanosized ordered mesoporous silica, followed by carbonization and removal of the silica template [11]. However, this hard-templating synthesis method is time-consuming, costly, and unsuitable for mass production. A reliable and facile strategy to synthesize OMCs without the use of a hard template is desirable. Based on this mind, lots of works have been made to obtain OMCs, for example, the organic-organic assembly method, which has been employed to synthesize OMCs by using amphiphilic triblock copolymers as a soft template and phenolic resol as a carbon source [12, 13]. Among these works, solvent evaporation induced self-assembly (EISA) process has been known as a powerful preparation route for ordered mesoporous carbonaceous films or powders. It can be carried out by solution casting on the planar substrates or the solid scaffold by evaporation, thermopolymerization, and carbonization to obtain the carbonaceous materials. In this way, by employing cigarette filters as the solid scaffold, the obtained materials can show much larger surface area and pore volume than that of scaffold carbon alone, which may result in enhanced adsorption performance.

Recently, Zhao's group prepared carbon-silica composite materials by EISA route using decomposable polyether polyol-based polyurethane (PU) foam scaffold [14]. Afterwards, this group prepares hierarchically porous carbonaceous monolith materials with 3-D cubic ($Im\bar{3}m$) and 2-D hexagonal ($p6mm$) mesostructure by using foam scaffold [15]. It is important to note that a well foam scaffold purchased plays a key role in the preparation of hierarchically ordered porous carbons (HOPC). However, it is time-consuming to obtain the foam scaffold, which needs to

allocate large resources to fabricate and produce lots of unfavourable residues to environment [16, 17]. In this case, it is also not an eco-friendly way for preparing HOPC by using plenty of PU foam. Cigarette filters, one of the most common solid wastes, are often thrown away in most cases. It is important task to reuse the solid wastes as a new resource. Nevertheless, carbonaceous materials obtained by carbonizing the used cigarette filters couldn't be widely used for its lower specific surface area and pore volume. In this paper, a strategy for the preparation of MCMs is presented by using solid wastes, cigarette filters as scaffold. The resulted materials obtained by employing EISA method incorporate the advantages of both cigarette filters and phenol/formaldehyde resol, and possess uniform pore structure, large surface area and pore volume, as well as exhibit a considerable CO_2 capture (2.48 mmol g^{-1}) and phenol adsorption (261.7 mg g^{-1}).

2. Experimental

2.1. Samples

Smoked cigarettes were collected, and the coating was separated from the remaining filter materials. The filters were washed with deionized water and dried for future use.

2.2. Experimental methods

2.2.1. *Preparation of carbonaceous materials:*

Preparation of the carbon precursor: The carbon precursor was prepared according to the literature [18]. For a typical procedure, phenol (6.1g, 65 mmol) was completely melted at 42 °C in a flask; then a 20 wt% NaOH solution (1.3 g, 32.5

mmol) was slowly added with stirring. After that, 37 wt % formalin (10.5 g, 130 mmol), which is an aqueous solution of formaldehyde, was added, and the mixture was heated at 70 °C for 1 h. After cooling to room temperature, the pH was adjusted to 7.0 by using 2.0 M HCl solution. After removing the water under vacuum, the product was dissolved in the ethanol (40 wt. %).

Preparation of the ordered mesoporous carbon (FDU-15): The ordered mesoporous materials were prepared according to the literature method [18]. Typical synthetic procedure as follows: triblock copolymer poly(ethyleneoxide)-b-poly(propylene oxide)-b-poly(ethylene oxide) (PEO-PPO-PEO, pluronic 127, 1.0 g) was dissolved in ethanol (20.0 g), then the carbon precursor containing phenol (0.61 g, 6.50 mmol) and formaldehyde (0.39 g, 13.0 mmol) was added into the solution and stirred for 10 min. After that, the solution was poured into a dish to evaporate the ethanol at room temperature over 8 h to obtain a transparent membrane. The membrane was then kept at 100 °C for 24 h to thermopolymerize the phenolic resins. The pyrolysis was carried out in a tubular furnace under N_2 atmosphere at 350 °C for 2 h and then 600 °C for 2 h with a ramp rate of 1 °C min^{-1}.

Preparation of the mesoporous carbonaceous materials (MCMs)*:* The mesoporous composites were prepared according to the literature method by employing the resol, F127 triblock copolymer and cigarette filters [15]. In a typical synthetic procedure, F127 (1.0 g) was dissolved in ethanol (8.5 g), and stirred at 40 °C for 1 h to afford a clear solution. The resol solution (2.5 g) of the above precursors was slowly added with stirring over 1 h. After that, amount of used cigarettes filters

were immersed the obtained homogeneous solution. The air bubbles inside the cigarettes filters were removed by squeezing the scaffolds with a glass rod. It took 8 h to evaporate the solvent at room temperature in the drafty closet, and 24 h at 100 °C in an oven for the further thermopolymerization. Mesoporous materials were obtained by carbonizing the as-made samples at 600 °C for 2 h in N_2 with a ramp rate of 1 °C min^{-1}.

Preparation of the porous carbonaceous materials (PCMs) using used cigarette filters: The PCMs were obtained by carbonizing the used cigarette filters without adding phenolic resins. The filters were carbonized at 600 °C for 2 h in N_2 with 1 °C min^{-1} heating rate.

2.2.2. *Adsorption performance of carbonaceous materials:*

Phenol adsorption measurements: Since phenol is toxic and corrosive, the experiments were done in a fume hood with wearing rubber gloves and gas mask. The adsorption performance of the three adsorbents (MCMs, FDU-15, PCMs) was investigated. In each adsorption experiment, 0.20 g adsorbent was added in 100 mL phenol solution with different initial phenol concentrations (100-700 mg L^{-1}). The resulting mixture was continuously stirred at 25 °C for a certain time until equilibrium was reached. The phenol concentration in the supernatant was analyzed with a UV spectrophotometer (UV-1700, Shimadzu), with the wavelength at 270 nm. Prior to the analysis, centrifugation was used to avoid potential interference from suspended scattering particles in the UV analysis. The amount of phenol adsorbed q_e (mg g^{-1}) was calculated as

$$q_e = V \cdot \frac{C_0 - C_e}{W} \quad (1)$$

where C_0 (mg L^{-1}) is the initial concentration of phenol solution, C_e (mg L^{-1}) is the equilibrium concentration of phenol solution, V (L) is the volume of the solution, and W (g) is the weight of the adsorbent. To determine C_e, the working curve of the UV absorbency of the phenol standard solution was first measured, then the absorbency of residual phenol solution was measured and C_e was calculated based on the working curve.

CO_2 capture measurements: The CO_2 adsorption measurements were carried out using Micrometitics TriStar 3020 volumetric adsorption analyzer at 25 °C and at the pressures of CO_2 from 0 to 101 kPa. The temperature was controlled by a circulating bath. Before measurement the samples were degassed at 120 °C in a vacuum for 24 h to remove any moisture and CO_2 molecules adsorbed in the pores.

2.3. Characterization techniques

Small-angle X-ray diffraction (XRD) patterns were collected using a Rigaku D/MAX-2500 X-ray diffraction system (Cu Kα radiation, λ=0.15406 nm) operated at 40 kV and 40 mA. Scanning electron microscopy (SEM) was performed on a HITACHI S-4800-I scanning electron microscope. The samples were mounted on an aluminum stub using adhesive carbon tape and SEM images were obtained at different magnifications. High-resolution Transmission electron micrographs (HR-TEM) were obtained on a JEOL JEM-2010 electron microscope. Samples for HR-TEM studies were prepared by placing a drop of the suspension of sample in ethanol onto a carbon-coated copper grid, followed by evaporating the solvent.

Nitrogen adsorption-desorption isotherm measurements were performed on a Micrometitics TriStar 3020 volumetric adsorption analyzer at -196 °C. The samples were degassed at 100 °C overnight before the measurement. The Brunauer-Emmett-Teller (BET) method was utilized to calculate the specific surface area of each sample and the average pore size distribution was derived from the desorption branch of the corresponding isotherm using the Barrett-Joyner-Halenda (BJH) method. The total pore volume was estimated from the N_2 amount adsorbed at a relative pressure of $P/P_0 = 0.97$. The specific surface area was calculated from the relative pressure of P/P_0 0.05 - 0.35.

3. Results and discussion

3.1. XRD characterization

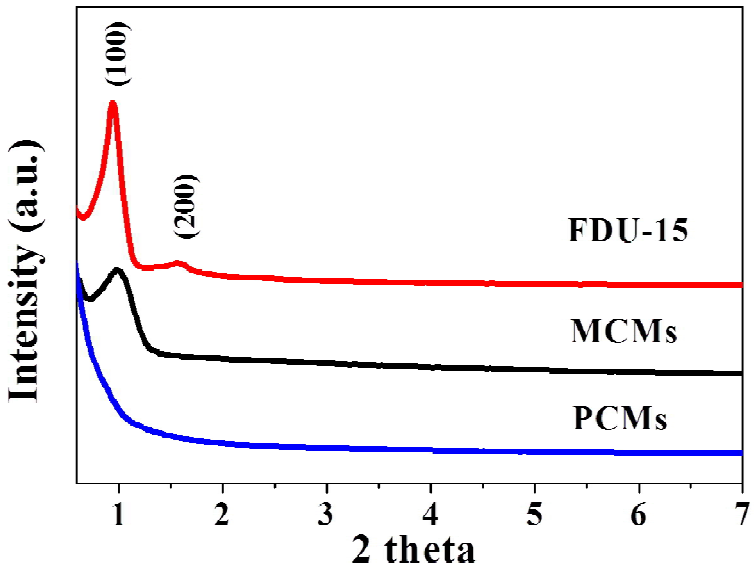

Fig. 1 XRD patterns of the carbon materials, MCMs, FDU-15 and PCMs.

The small-angle X-ray diffraction (XRD) patterns of the carbon materials are shown in the Fig 1. It shows that FDU-15 has two well-defined diffraction peaks

which can be indexed as (100) and (200) reflections of 2D hexagonal (*p6mm*) symmetry, indicating a highly ordered mesostructure [18]. In comparison, MCMs show a less resolved diffraction peak due to the introduction of disordered cigarette filers carbon. Only one diffraction is shown in the MCMs. According to the literature, the diffraction could be indexed as (100) reflections of a 2D hexagonal mesostructure (*p6mm* space group) [18, 19]. It suggests the products obtained are imperfect with a degradation of the ordered mesostructure, which may contain the ordered mesostructured carbonaceous shells and amorphous cigarette filters carbon. It also shows that the ordered mesostructure of MCMs is thermally stable during the carbonization process [14, 18]. The ordered mesostructure is perfectly retained, despite the removal of a large part of the template on the calcination.

3.2. SEM and TEM characterization

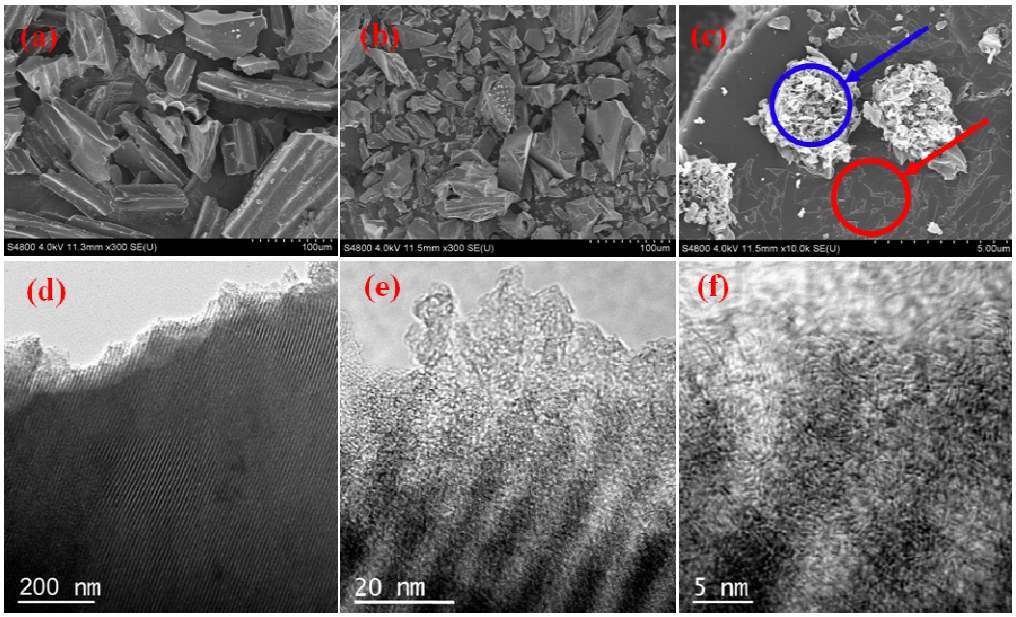

Fig. 2 SEM images of PCMs (a) and MCMs (b and c), TEM images (d, e, f) of MCMs

The scanning electron microscopy (Fig. 2 (a, b, c)) images show that the struts of the carbonaceous materials are not hollow, but irregular rods with some grooves. SEM image of PCMs (Fig. 2a) fabricated by used cigarette filters shows that several impurities appear on the surface of the irregular rods, which result from residual impurities of tobacco burning. As shown in Fig. 2c, abundant phenolic resins carbon (red circle part) coats on the surface of MCMs. It is noted that their surface transforms into folds structure for the presence of schistose carbonaceous materials, which come from the polymerization and carbonization of phenolic resins. Besides, it also shows the presence of residual impurities (blue circle part). Transmission electron microscopy (TEM) images reveal more-refined structural features. The MCMs show large domains of stripe-like patterns (Fig. 2d), further confirming the ordered mesostructure. Besides, lots of micropores appear on the edges of carbonaceous materials or the walls of mesoporous channels (Fig. 2e and f), that is to say, the main mesoporous channels are interconnected through micropores inside the walls of the main channels, which is beneficial for CO_2 capture [20].

3.3. N_2 adsorption-desorption measurements

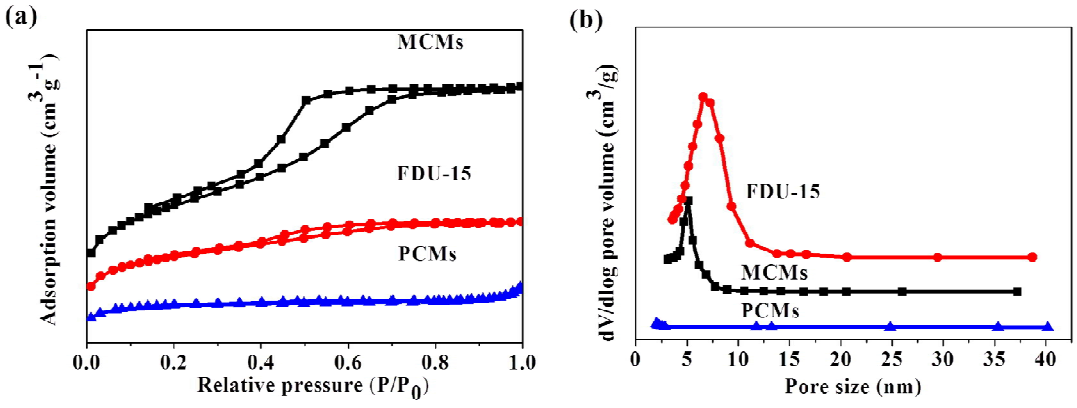

Fig. 3 N_2 sorption isotherms and pore size distribution of MCMs, FDU-15 and PCMs.

N_2 sorption isotherms of the carbon materials are shown in Fig. 3. It can be seen that FDU-15 and MCMs both exhibit representative type IV curves with obvious capillary condensation steps at P/P_0=0.4-0.75 (Fig. 3a), which is consistent with the literature [15, 18]. The adsorption and desorption branches of MCMs deviate at low relative pressure, which is related to the asymmetric shrinkage of pores [15]. Compared with FDU-15, the capillary condensation step of MCMs is shifted slightly to lower relative pressure, which is related to the slight reduction in aperture size to 5.1 nm, resulting from framework shrinkage [15]. MCMs shows a BET surface area of 526 $m^2 g^{-1}$ and a narrow pore size distribution with a mean value of 5.1 nm calculated from the adsorption barch based on BJH model (Table 1). The H_1 hysteresis loop of MCMs suggests that it has imperfect cylindrical channels, implying the presence of partial asymmetric pore shrinkage [14]. Compared with PCMs and FDU-15, an increase in the surface area (526 $m^2 g^{-1}$) and pore volume (0.39 $cm^3 g^{-1}$) of MCMs is obtained after the template is further removed. This can be attributed to the formation of micropores resulted from cigarette filters carbonization or the edges of carbonaceous materials and the walls of mesoporous channels [21].

Table 1 Pore structure parameters of MCMs, FDU-15, PCMs; S_{BET} is the specific surface area, D_{BJH} is the pore diameter, V_{BJH} is the total pore volume and the capacity of CO_2 capture

Sample	S_{BET} ($m^2 g^{-1}$)	V_{pore} ($cm^3 g^{-1}$)	D_{pore} (nm)
MCMs	526	0.39	5.1
FDU-15	460	0.22	6.6
PCMs	296	0.18	—

3.4. Phenol adsorption measurements

3.4.1 Effect of contact time and various concentration on phenol removal

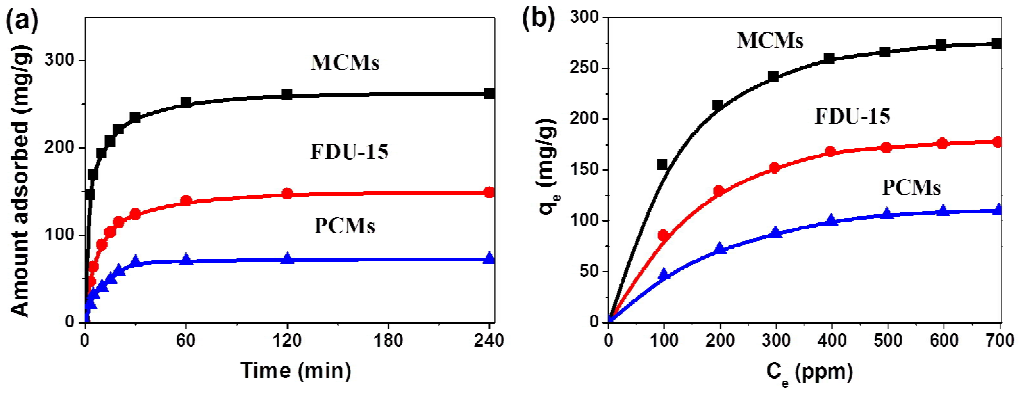

Fig. 4 Effect of contact time (a) and various initial phenol concentrations (b) on the phenol adsorption over MCMs, FDU-15 and PCMs.

Fig. 4 depicts the effect of contact time and various phenol concentrations on the removal of phenol over three adsorbents. In the Fig. 4a, the saturation curves rise sharply in the initial stages, indicating that there are plenty of readily accessible sites. Element analysis shows that the samples are mainly composed of carbon, with small amount of hydrogen and oxygen. Such faster adsorption kinetics for phenol removal is related to the hydrogen bonding between hydroxyl groups of phenols and porous carbon surface [22]. Eventually, a plateau is reached in all curves indicating that the adsorbent is saturated at this level. It can be seen from Fig. 4a that the removal curves are single, smooth and continuous, indicating the formation of monolayer coverage of the phenol molecules onto the outer surface of the adsorbent [23]. In the Fig. 4b, the adsorption isotherms are obtained after adsorption for 12 h. The phenol adsorbed capacity of MCMs is much higher than that of PCMs and FDU-15 for the experimental conditions, suggesting the high efficiency of the MCMs, which is

attributed to the large surface area and pore volume of MCMs [23]. After 6 adsorption-desorption cycles, the performance is reduced to 86%. It is noteworthy that there were no significant difference in the adsorption capacity between new cigarette filters and used cigarette filters. In other words, the existence of tar has little influence on the result of the whole adsorption. Furthermore, the filters were washed to remove the attached tiny dust, and it shows better performance than non-washed filters.

3.4.2 Adsorption isotherms

Adsorption isotherm is important to describe how solutes interact with adsrobents, and is critical in optimizing the use of adsrobents. As shown in Fig. 5, the adsorption isotherms have been plotted to follow the Langmuir and Freundlich equation. Langmiur model is based on the assumption of homogeneous adsorbent surface with identical adsorption sites and no transmigration in the plane of the surface [24], which can be expressed as:

$$\frac{C_e}{q_e} = \frac{C_e}{Q_0} + \frac{1}{Q_0 \cdot b} \quad (2)$$

Where, C_e is the equilibrium concentration of adsorption (mg L^{-1}), q_e is the amount of absorbate adsorbed (mg g^{-1}), Q_0 is the Langmiur constant (the maximum adsorption amount), b is the Langmiur constant (L mg^{-1} or L mol^{-1}). Therefore, the Q_0 can be obtained from the reciprocal of the slope of a plot of C_e/q_e against C_e. The Q_0 values that are determined from Fig. 5 are summerised in Table 2.

Freundlich model is an emprical equation assuming heterogeneous adsorptive energies on the surface, which are shown as [25]:

$$q_e = K_F C_e^{1/n} \quad (3)$$

Where, K_F and n are Freundlich constants related to the adsorption amount and intensity, respectively.

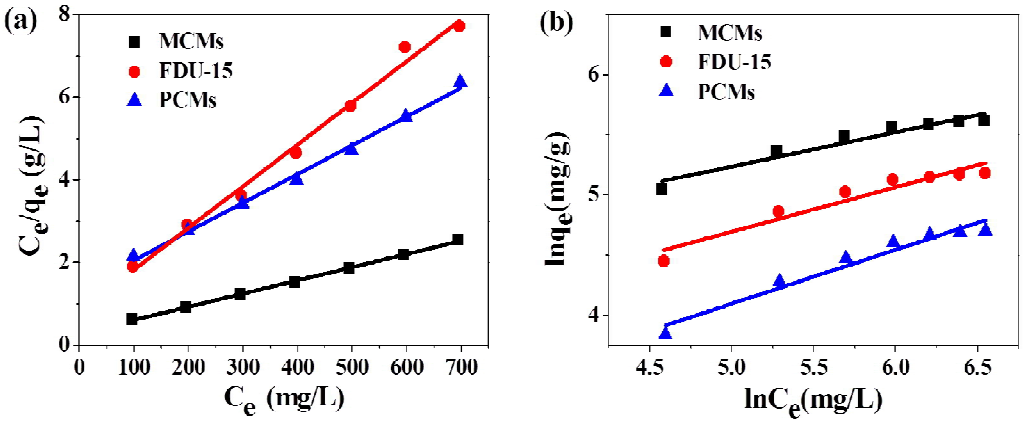

Fig. 5 (a) the Langmuir isotherms of phenol adsorption over three adsorbents; (b) the Freundlich isotherms of phenol adsorption over MCMs, FDU-15 and PCMs.

Table 2 Isotherms constants for adsorption of phenol over MCMs, FDU-15 and PCMs.

Adsorbent	Langmuir			Freundlich		
	Q_0 (mg/g)	b (L/mg)	R^2	K_F ((mg/g)(L/mg)$^{1/n}$)	n	R^2
MCMs	257.5	0.19	0.998	45.02	3.502	0.947
FDU-15	143.9	0.11	0.994	17.17	2.704	0.920
PCMs	99.1	0.05	0.990	6.39	2.232	0.911

The paraments are also calculated and summerised in Table 2. It can be seen that the Langmuir isotherms of three adsorbents fit quite well with the experimental data, compared to the Freundlich isotherms which have lower correlation coefficients. This is comparable to the result for the phenol adsorption on activated carbon reported in the literature [25]. Besides, compared to the other adsorbents, MCMs exhibits much

larger monolayer adsorption capacity (257.5 mg g^{-1}) of phenol, which is 2.59 and 1.79 times of that over PCMs and FDU-15, respectively. This should be attributed to its large surface area and large pore volume [23]. It should also be noted that the MCMs show the best adsorption capacity of phenol among the adsorbents reported in the literature (1.48-165.80 mg g^{-1}) [26-28].

3.4.3 Adsorption kinetics

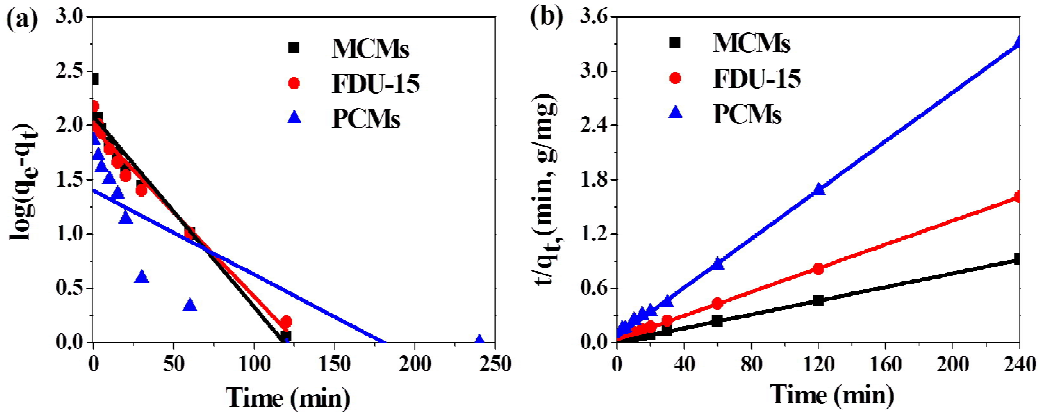

Fig. 6 (a) the plots of pseudo-first-order kinetics of phenol adsorption over three adsorbents, (b) the curves of pseudo-second-order kinetics of phenol adsorption over MCMs, FDU-15 and PCMs. (C_i: 400 ppm)

The adsorption kinetics curves of the phenols are shown in Fig. 6. The kinetics are fitted with the pseudo-first-order and pseudo-second-order models, which are extensively used in kinetic studieds. The pseudo-first-order model can be expressed as [29] :

$$\ln(q_e - q_t) = \ln q_e - k_1 t \quad (4)$$

Where k_1 is the first-order rate constant. The values of $\ln(q_e - q_t)$ are calculated from the experimental data and plotted against t, k_1 is the calculated from the slope of the plot.

The pseudo-second-order model is shown as [30]:

$$\frac{t}{q_t} = \frac{1}{k_2 \cdot q_e^2} + \frac{t}{q_e} \quad (5)$$

where k_2 is the second-order rate constant. The values of t/q_t are plotted against t, q_e and k_2 are calculated from the slope and intercept of the plot.

Table 3. Comparison of the pseudo-first-order and pseudo-second-order adsorption rate constants, and calculated and experimental q_e values over MCMs, FDU-15 and PCMs.

Adsorbent	q_e, exp(mg/g)	**Pseudo-first-order**			**Pseudo-second-order**		
		k_1	R^2	q_e, cal (mg/g)	k_2	R^2	q_e, cal (mg/g)
MCMs	261.7	0.418	0.952	120.79	0.039	0.997	265.3
FDU-15	148.9	0.327	0.965	93.86	0.026	0.996	152.7
PCMs	72.4	0.172	0.616	25.08	0.019	0.992	74.2

The adsorption constants of two models over three adsorbents are listed in Table 3. It can be seen that the pseudo-first-order model gives poor fitting with low R^2 values and notable variances between the experimental and theoretical uptakes. The pseudo-second-order fits the experimental data well for all phenols. The R^2 values are close to unity and the experimental and theoretical uptakes are in good agreement, which is agreed with the report that the pseudo-second-order models are suitable for

the adsorption of lower molecular weight adsorption on smaller adsorption particles [31].

3.5. CO_2 adsorption measurements

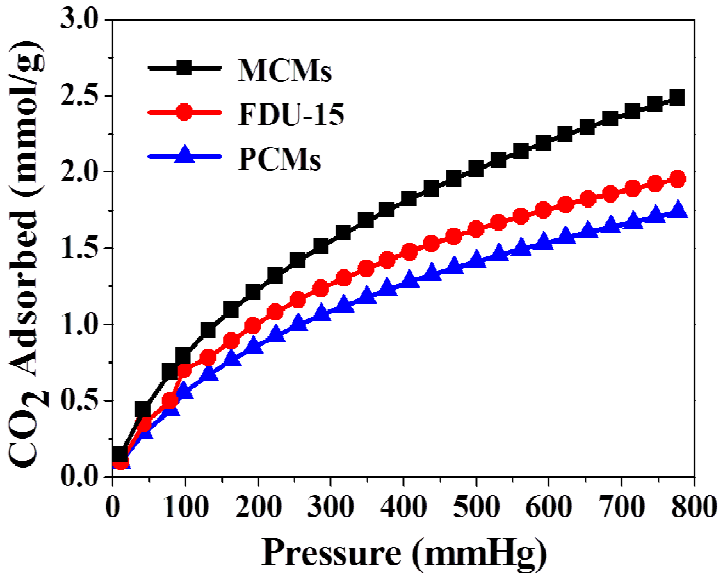

Fig. 7 Adsorption isotherms of MCMs, FDU-15 and PCMs for CO_2 capture at 25°C.

The capture of CO_2 has attracted considerable attention in recent years because it is the main anthropogenic contributor to climate change. A comparative analysis of CO_2 adsorption isotherms (measured at 25 °C and 1.0 bar) of the three carbonaceous materials is presented in Fig. 7. It can be seen that the CO_2 adsorption capacities of the MCMs with large surface area (526 $m^2 g^{-1}$) is 2.48 mmol g^{-1}. The value is higher than or at least comparable with those of reported N-dope porous carbon for CO_2 adsorption [6, 32]. By contrast, PCMs and FDU-15 only show CO_2 capacities of 1.74 mmol g^{-1} and 1.95 mmol g^{-1} with a surface area of 296 m^2 g^{-1} and 460 m^2 g^{-1}, respectively. It should be noted that, the MCMs displays much larger pore volume (see Table 1) than that of FDU-15 and PCMs. This demonstrates that large surface

area and pore volume are of benefit to CO_2 capture. Some previous researches have also reported that microporosity in the materials is beneficial for CO_2 capture and storage [33, 34]. This is due to the statement that micropores have a high adsorption potential that enhances the adsorption performance of CO_2 molecules [23]. Besides, pore channels with high specific surface area and large pore volume can accelerate the diffusion and interaction of CO_2 molecules during the sorption process [35]. This is confirmed by the CO_2 capture performance of MCMs. In addition, no saturation is observed up to a pressure of 1.0 bar, suggesting that higher CO_2 adsorption capacity can be achieved at a higher pressure.

4. Conclusions

Porous carbon materials with ordered mesostructure are prepared successfully by using the EISA method with phenol/formaldehyde resol as carbon precursor, triblock copolymer F127 as mesostructural template and cigarettes filters as carbon matrix scaffold. The resulted products possess an ordered *p6mm* mesostructure, large surface area and uniform pore size. In addition, it is noted that the MCMs incorporate the advantages of ordered mesostructured carbon and amorphous cigarette filters carbon. The obtained materials have exhibited a considerable performance for phenol adsorption (261.7 mg g^{-1}) and CO_2 capture (2.48 mmol g^{-1}), which provides a new way for the recycling of solid wastes, cigarette filters.

Acknowledgements

This work was financially supported by the Natural Science Foundation of China (20906019), Science and Technology Research Projects in Hebei Universities

(QN20131069, QN2014142, ZD20131032 and Z2013001), and Five Platform Open Fund Projects of Hebei University of Science and Technology (2014PT86).

References

[1] E.A. Smith and T.E. Novotny, *Tobacco Control.*, 2011, **20**, 2–9.

[2] E.T. Novotny, S.N. Hardin, L.R. Hovda, D.J. Novotny, M.K. McLean and S. Shan, *Tobacco Control.*, 2011, **20** (Suppl.1), 17–20.

[3] Yazdi S. Kazemi, Soltani S. Masoudi and S. Hossein, *Adv. Mater. Res.*, 2012, **587**, 88–92.

[4] S. Polarz, B. Smarsly and J.H. Schattka, *Chem. Mater.*, 2002, **14**, 2940–2495.

[5] W. Li, Q. Yue, Y. Deng and D. Zhao, *Adv. Mater.*, 2013, **25**, 5129–5152.

[6] J. Wei, D. D. Zhou, Z. K. Sun, Y. H. Deng, Y. Y. Xia and D. Y. Zhao, *Adv. Funct. Mater.*, 2013, **23**, 2322–2328.

[7] M. Barczak, K. Michalak-Zwierz, K. Gdula, K. Tyszczuk-Rotko, R. Dobrowolski and A. Dabrowski, *Micropor. Mesopor. Mater.*, 2015, **211**, 162–173.

[8] H. Liu, W. Cui, L.Jin, C. Wang and Y. Xia, *J. Mater. Chem.*, 2009, **19**, 3661–3667.

[9] Q. Shi, R. Zhang, Y. Lv, Y. Deng, A. A. Elzatahrya and D. Zhao, *Carbon*, 2015, **84**, 335-346.

[10] K. Kwon, Y. Sa, J. Cheon and S. Joo, *Langmuir*, 2012, **28**, 991–996.

[11] G. Mane, S. Talapaneni,, C. Anand S. Varghese, H. Iwai and Q. Ji, et al. *Adv. Funct. Mater.*, 2012, **22**, 3596-3604.

[12] C. Liang and S. Dai, *J. Am. Chem. Soc.*, 2006, **128**, 5316–5317.

[13] F. Zhang, D. Gu, T. Yu, F. Zhang, S. Xie and L. Zhang, et al. *J. Am. Chem. Soc.*,

2007, **129**, 7746–7747.

[14] C. Xue, B. Tu and D. Zhao, *Adv. Funct. Mater.*, 2008, **18**, 3914–3921.

[15] C. F. Xue, B.Tu and D. Y. Zhao, *Nano Res.*, 2009, **2**, 242–253.

[16] G. Behrendt and B. Naber, *Metallurgy*, 2009, **4**4, 3–23.

[17] JH. Janik and M. Marzec, *Mater. Sci. Eng. C*, 2015, **48** , 586–591.

[18] Y. Meng, D. Gu, F. Zhang, Y. Shi and H.Yang, Z. Li, et al. *Angew. Chem. Int. Ed.*, 2005, **44**, 7053–7059.

[19] D. Y. Zhao, J. L. Feng, Q. S. Huo, N. Melosh, G. H. Fredrickson, B. F. Chmelka and G. D. Stucky, *Science*, 1998, **279**, 548-52.

[20] L. Wang and R. Yang, *J. Phys. Chem. C*, 2011, **115**, 21264–21272.

[21] G. Chandrasekar, W. Son and W. Ahn, *J. Porous Mater.*, 2009, **16**, 545–551.

[22] J. He, K. Ma, J. Jin, Z. Dong, J. Wang and R. Li, *Micropor. Mesopor. Mater.*, 2009, **121**, 173-177.

[23] B. Hameed and A. Rahman, *J. Hazard. Mater.*, 2008, **160**, 576–581.

[24] K. Hall, L. Eagleton, A. Acrivos and T. Vermeulen, *Ind. Eng. Chem. Fundam.*, 1996, **5**, 212–223.

[25] H. Freundlich, *J. Phys. Chem.*, 1906, **5**7, 385–470.

[26] I. Vázquez, J. Rodríguez-Iglesias, E. Marañón, L. Castrillón and M. Álvarez, *J. Hazard. Mater.*, 2007. **147**. 395–400.

[27] A. Kumar, S. Kumar and D. Gupta, *J. Hazard. Mater.*, 2007, **147**, 155–166.

[28] B. Özkaya, *J. Hazard. Mater.*, 2006, **129**, 158–163.

[29] E. Tutem, R. Apak and C. Unal, *Water Res.*, 1998, **32**, 2315–2324.

[30] E. Haque, J. Jun, S. Talapaneni, A. Vinu and S. hung, *J. Mater. Chem.*, 2010, **20**, 10801–10803.

[31] F. Wu, R. Tseng, S. Huang and R. Juang, *Chem. Eng. J.*, 2009, **151**, 1–9.

[32] G. Hao, Z. Jin, Q. Sun, X. Zhang, J. Zhang and A. Lu, *Energy Environ. Sci.*, 2013, **6**, 3740-3747.

[33] V. Zelenak, D. Halamova, L. Gaberova, E. Bloch and P. Llewellyn, *Micropor. Mesopor. Mater.*, 2008, **116**, 358-364.

[34] C. Martín, M. Plaza, S. García, J. Pis, F. Rubiera and C. Pevida, *Fuel*, 2011, *90*, 2064-2072.

[35] H. Yang, Y. Yuan and S. Tsang, *Chem. Eng. J.,* 2012 *185-186*, 374–379.

TOC Graphic

Mesoporous carbonaceous materials (MCMs) are synthesized by using resol as the carbon precursor, triblock copolymer F127 as the template and cigarette filters as the matrix scaffold, which exhibit a considerable phenol adsorption (261.7 mg g^{-1}) and CO_2 capture (2.48 mmol g^{-1}).

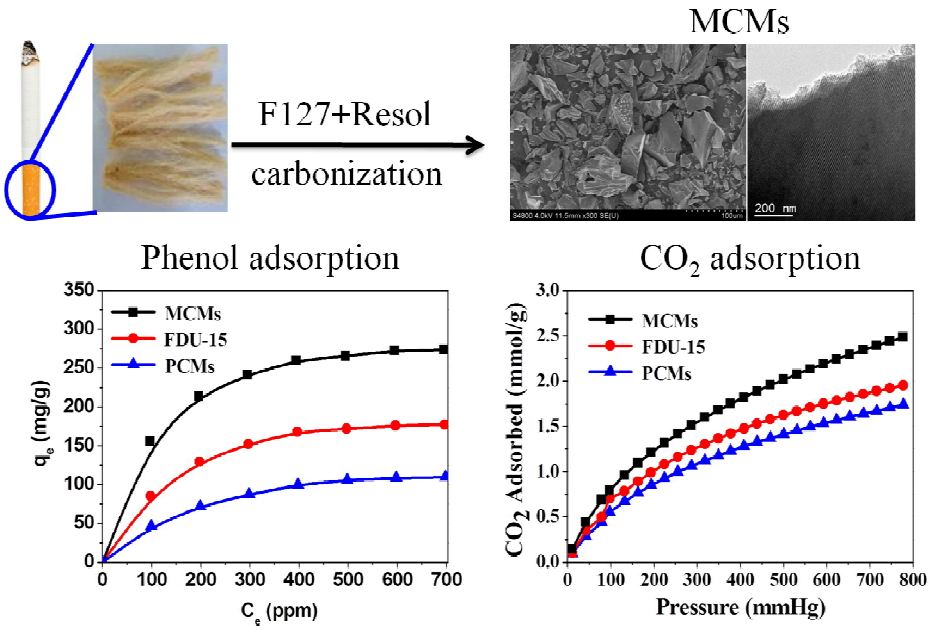

Highlights

- Mesoporous carbonaceous materials with 2-D hexagonal (*p6mm*) are obtained.
- Cigarette filters, the solid wastes, are used as matrix scaffold.
- The carbon materials obtained show a large specific surface area.
- The carbon materials show a considerable phenol adsorption and CO_2 capture.
- It provides a new way for the recycling of solid wastes.